Analysis of Pleistocene paleodrainage evolution in the Po Basin (Italy) by multivariate statistical techniques

G. Vezzoli
University of Milano-Bicocca, Milano, IT; *giovanni.vezzoli@unimib.it*

Abstract

In order to obtain a high-resolution Pleistocene stratigraphy, eleven continuously cored boreholes, 100 to 220m deep were drilled in the northern part of the Po Plain by Regione Lombardia in the last five years. Quantitative provenance analysis (QPA, Weltje and von Eynatten, 2004) of Pleistocene sands was carried out by using multivariate statistical analysis (principal component analysis, PCA, and similarity analysis) on an integrated data set, including high-resolution bulk petrography and heavy-mineral analyses on Pleistocene sands and of 250 major and minor modern rivers draining the southern flank of the Alps from West to East (Garzanti et al, 2004; 2006). Prior to the onset of major Alpine glaciations, metamorphic and quartzofeldspathic detritus from the Western and Central Alps was carried from the axial belt to the Po basin longitudinally parallel to the SouthAlpine belt by a trunk river (Vezzoli and Garzanti, 2008). This scenario rapidly changed during the marine isotope stage 22 (0.87 Ma), with the onset of the first major Pleistocene glaciation in the Alps (Muttoni et al, 2003). PCA and similarity analysis from core samples show that the longitudinal trunk river at this time was shifted southward by the rapid southward and westward progradation of transverse alluvial river systems fed from the Central and Southern Alps. Sediments were transported southward by braided river systems as well as glacial sediments transported by Alpine valley glaciers invaded the alluvial plain.

Kew words: Detrital modes; Modern sands; Provenance; Principal Components Analysis; Similarity, Canberra Distance; palaeodrainage.

1 Introduction

Foreland basins are comprehensive stratigraphic archives, from which any detail of the geological history of associated orogens can be potentially retrieved by quantitative provenance analysis of sedimentary successions (QPA, Weltje and von Eynatten, 2004; von Eynatten 2004). Trends in sediment composition cannot be safely interpreted as documenting paleotectonic events whenever paleodrainage shifts represent an equally reasonable alternative. Understanding drainage evolution is thus a fundamental step to correctly unravel the interactions between tectonic and climatic processes which control the erosional evolution of mountain belts. In this study I focus on well-studied Quaternary subsurface sequences of the Lombardy Po Plain (Carcano and Piccin, 2002, Garzanti et al., 2004, 2006) to illustrate a quantitative method of paleodrainage analysis. Pleistocene sediments of the Po Basin represent an excellent natural laboratory in which to use statistical analysis to investigate how sediment composition reflects climate changes (Muttoni et al., 2003) and to reconstruct the Alpine palaeodrainage patterns (Vezzoli and Garzanti, 2008). This method, based on modern analogues, can be performed by comparing detrital modes of modern and Pleistocene sands by principal component analysis (PCA) and similarity analysis. PCA was used to define petrographic end-members for each core. Successively, these end-members were compared with the modern-sand database and analysis of similarity was used in order to evaluate the goodness of fit of a model. Finally, I reconstructed the major changes of palaeodrainage and foreland-basin fills with the onset of the first major glaciation in the Alps.

2 Geological background

The Po Basin represents the foredeep of the Southern Alps and the Apennines (Fig. 1) and since the Late Oligocene detritus from the Alpine chain with contrasting provenance signatures was carried down into the alluvial Plain (Gonfolite Group, Garzanti and Malusà, 2008). At the beginning of the Quaternary, climatic control on sediment budget became predominant (Muttoni et al. 2003; Scardia et al., 2006), and with the onset of Earth's global cooling, indicated in the ODP677 - SPECMAP, the Po Plain became a periglacial basin.

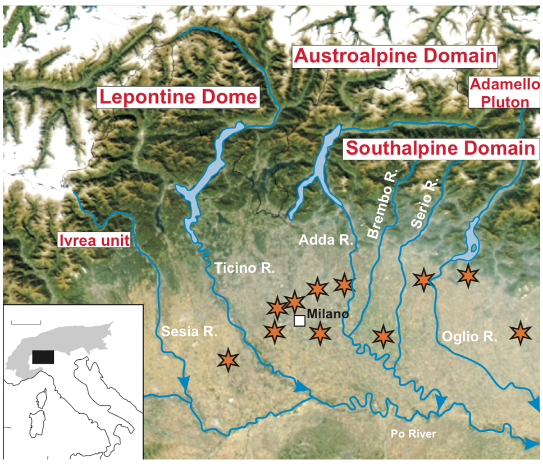

Figure 1: Map of the western Po Plain. Stars indicate location of 11 Regione Lombardia cores

3 Methods

A paleodrainage analysis based on modern analogues can be performed by comparing detrital modes of modern and Pleistocene sands by multivariate statistical techniques. With the basic assumption that in the last million years neither source-area geology nor river-sediment composition have changed significantly, we considered the present composition of Alpine tributaries of the Po River as primary end-member sources of detritus for Pleistocene deposits. Apenninic tributaries can be disregarded because provenance analysis of all eleven core sections showed that the paleoPo was flowing south of the Lombardy study area during the Late Quaternary. For paleodrainage analysis to be sufficiently precise, detrital modes of primary end-members were obtained by integrated high-resolution petrographic-mineralogical analysis of three to six replicate samples for each modern river. Samples were collected by different operators, in different years, different seasons, and different localities at the Southalpine front and upstream of major lakes, in order to average out variations related to diverse factors including seasonal changes (Weltje, 2004).

3.1 Sampling

48 sediment samples were collected from eleven continuously cored boreholes (100 to 220m deep) drilled in the northern part of the Po Plain by Regione Lombardia in the last ten years (Fig. 1). 21 samples were collected parallel to the Southalpine margin (cores RL1-Ghedi, RL4-Agrate, RL5-Trezzo, RL6-Cremignane and RL7 Palosco) whereas 27 samples were collected more basinward (cores RL2-Pianengo, RL3-Cilavegna, RL8-Peschiera Borromeo, RL9-Gaggiano, RL10-Triulza and RL11 Parco Nord). On each core magnetostratigraphy has been used to date Pleistocene sediments (Muttoni et al., 2003; Scardia et al., 2006).

3.2 Analytical protocols and compositional parameters

Each sample consists of 200g of the whole sand fraction. Thin sections were stained with alizarine red to distinguish dolomite and calcite, and on each section 400 points were counted by the Gazzi-Dickinson point-counting method (Ingersoll et al. 1984; Zuffa 1985, Table 1). A very detailed classification scheme allowed us to collect full quantitative information on coarse-grained rock fragments, and thus to recalculate also traditional QFR parameters from the data set obtained, meeting all possible needs (Suttner and Basu, 1985). Metamorphic rocks fragments were classified according to four protolith compositions, each subdivided into five ranks (Garzanti and Vezzoli, 2003). For each sample, mean rank is expressed by a Metamorphic Index (MI), ranging from 100 (only very-low rank grains, such as slate) to 500 (only very-high rank grains, such as coarse-grained gneiss). Pure marble grains could not be consistently distinguished from recrystallized sparites, and were included with carbonate grains (Lc). Impure calcschist grains were split equally between carbonate (Lc) and metamorphic (Lm) grains. Heavy minerals were concentrated with sodium metatungstate (density 2.9 g/cm^3), using the 63-250-micron fraction. This fraction was treated with oxalic and acetic acids to eliminate iron oxides and carbonates, respectively (Parfenoff et al., 1970). On each sample, 250 transparent dense minerals were counted on grain mounts by the ribbon-counting methods (Mange and Maurer, 1992; Tables A1-A2). Median grain size was determined with sieving techniques. The abundance of transparent heavy minerals in the sediment, expressed by the transparent Heavy Mineral Concentration (tHMC index; Garzanti and Andò, 2007) were used to collect quantitative information on protolith composition of source rocks. The Hornblende Color Index (HCI; Garzanti et al. 2004) was used to estimate the average metamorphic grade of metasedimentary and metaigneous source rocks, respectively. They vary from 0 in detritus from greenschist-facies to lowermost amphibolite-facies rocks yielding chloritoid and blue/green amphibole, to 100 in detritus from granulite-facies rocks yielding sillimanite and brown hornblende.

Table 1. Petrographic and mineralogical data of the Pleistocene detritus of the Po Basin cores.

core	depth	tHMC	MI	HCI	quartz	k-feldspar	plagioclase	volcanic lithic grains	limestone	dolostone	siltstone	chert	metamorphic lithic grains	serpentinite	muscovite	biotite	opaques	apatite	hornblende	glaucophane	tremolite	clinopyroxene	orthopyroxene	spinel	epidote	garnet	staurolite	andalusite	sillimanite	Tot.
Ghedi	26.3	0	46	20	12.4	0.4	3.4	8.6	25.0	36.0	5.3	4.9	1.5	0.4	0.2	0.2	1.4	0.0	0.3	0.0	0.0	0.0	0.0	0.0	0.1	0.0	0.0	0.0	0.0	100.0
Ghedi	35.9	4	93	11	34.5	5.3	12.3	7.7	12.1	12.4	3.5	0.9	3.5	0.7	0.7	1.1	1.6	0.1	3.0	0.0	0.0	0.2	0.0	0.0	0.3	0.2	0.0	0.0	0.0	100.0
Ghedi	47.9	1	272	11	63.7	2.4	4.3	1.9	6.1	0.0	1.5	0.4	15.6	0.0	0.6	1.3	1.0	0.0	0.3	0.0	0.0	0.0	0.0	0.0	0.2	0.5	0.1	0.0	0.1	100.0
Ghedi	49.6	2	187	32	45.5	1.8	6.5	17.4	4.0	5.8	0.8	0.4	12.3	0.0	1.9	0.6	1.4	0.2	0.2	0.1	0.0	0.0	0.0	0.0	0.4	0.5	0.0	0.0	0.1	100.0
Ghedi	59.6	2	227	12	52.2	1.4	4.4	7.2	14.1	2.6	1.5	0.0	11.9	0.0	1.1	0.6	1.6	0.0	0.6	0.0	0.0	0.0	0.0	0.0	0.2	0.5	0.0	0.0	0.0	100.0
Ghedi	71.8	0	72	27	5.2	0.3	1.3	2.9	41.2	46.1	0.8	1.3	0.0	0.0	0.7	0.0	0.2	0.0	0.0	0.0	0.0	0.0	0.0	0.0	0.0	0.0	0.0	0.0	0.0	100.0
Ghedi	90.5	1	262	28	53.1	3.3	7.9	1.0	0.5	1.0	0.7	0.0	11.2	1.0	13.0	5.8	0.4	0.0	0.4	0.1	0.2	0.0	0.0	0.0	0.3	0.1	0.0	0.0	0.1	100.0
Pianengo	11.5	5	278	32	57.9	6.2	10.6	3.3	1.5	0.7	0.7	0.0	9.5	1.8	0.2	0.9	1.9	0.1	1.7	0.0	0.1	0.3	0.0	0.0	0.7	1.2	0.2	0.0	0.4	100.0
Pianengo	38.3	1	186	15	57.2	5.3	10.5	3.8	3.8	0.4	4.1	0.0	10.5	0.0	1.7	1.3	0.5	0.0	0.5	0.0	0.0	0.0	0.0	0.0	0.2	0.2	0.0	0.0	0.0	100.0
Pianengo	39.9	4	240	14	37.7	3.0	11.7	5.3	18.8	4.5	0.4	0.0	9.0	0.4	1.5	2.3	1.2	0.0	2.4	0.0	0.0	0.0	0.0	0.0	0.4	0.6	0.0	0.8	0.1	100.0
Pianengo	44	2	233	16	44.6	3.1	8.1	4.7	5.2	8.4	2.5	0.0	17.1	0.0	1.6	1.6	0.9	0.0	0.9	0.0	0.0	0.1	0.0	0.0	0.3	0.4	0.2	0.2	0.1	100.0
Pianengo	63	0	139	21	14.2	0.4	1.1	5.1	37.6	35.0	2.6	1.0	2.2	0.0	0.0	0.0	0.3	0.0	0.1	0.0	0.0	0.0	0.0	0.0	0.1	0.3	0.0	0.0	0.0	100.0
Pianengo	80.6	1	186	15	38.6	1.2	4.2	7.5	14.4	10.7	2.6	1.9	16.1	0.7	0.4	0.0	1.0	0.0	0.3	0.0	0.0	0.0	0.0	0.0	0.2	0.2	0.0	0.0	0.0	100.0
Cilavegna	19.9	8	313	22	35.0	7.7	21.4	0.0	1.3	1.3	0.0	0.0	6.6	0.4	8.8	8.8	1.2	0.1	2.8	0.0	0.0	0.2	0.0	0.0	1.3	2.3	0.1	0.1	0.4	100.0
Cilavegna	61.8	8	329	26	49.2	6.0	16.8	0.0	0.0	0.0	0.0	0.0	8.4	1.6	4.4	4.4	1.4	0.1	2.8	0.0	0.3	0.2	0.0	0.0	1.2	2.7	0.2	0.0	0.4	100.0
Cilavegna	61.8	8	403	26	50.3	8.1	18.5	0.0	0.0	0.0	0.0	0.0	6.4	0.3	2.5	5.1	1.3	0.1	2.6	0.0	0.3	0.2	0.0	0.0	1.2	2.5	0.2	0.0	0.4	100.0
Agrate	10.8	1	211	42	28.5	13.2	12.5	2.5	14.5	7.2	1.1	3.6	8.6	0.7	2.7	3.7	0.5	0.0	0.5	0.0	0.0	0.0	0.0	0.0	0.1	0.1	0.0	0.0	0.0	100.0
Agrate	29.2	3	362	5	41.9	14.1	15.1	0.0	1.2	0.0	0.5	0.0	10.0	2.4	1.9	9.4	0.6	0.2	1.4	0.0	0.1	0.0	0.0	0.0	0.4	0.5	0.1	0.0	0.1	100.0
Agrate	36.7	0	188	15	43.4	3.8	3.8	7.1	20.1	0.0	2.2	11.5	5.7	0.3	0.5	0.8	0.2	0.0	0.1	0.0	0.0	0.0	0.0	0.0	0.1	0.1	0.2	0.0	0.0	100.0
Agrate	42.5	3	314	19	45.5	13.2	10.0	1.4	0.0	0.0	0.0	0.0	14.9	3.2	4.3	3.9	0.9	0.1	1.2	0.0	0.1	0.1	0.0	0.0	0.5	0.7	0.1	0.0	0.1	100.0
Trezzo	14.7	0	102	37	35.8	1.9	2.2	21.7	12.4	0.0	2.0	0.3	22.6	0.0	0.3	0.3	0.4	0.0	0.0	0.0	0.0	0.0	0.0	0.0	0.0	0.0	0.0	0.0	0.0	100.0
Trezzo	21.4	0	75	28	18.1	1.6	0.3	3.2	56.9	0.4	11.7	2.2	4.9	0.0	0.3	0.0	0.3	0.0	0.0	0.0	0.0	0.0	0.0	0.0	0.0	0.0	0.0	0.0	0.0	100.0
Trezzo	45.7	0	82	5	31.1	0.3	0.9	11.5	35.9	1.1	5.9	0.0	11.2	0.0	0.9	0.3	0.6	0.0	0.0	0.0	0.0	0.0	0.0	0.0	0.0	0.0	0.0	0.0	0.0	100.0
Trezzo	54.6	2	187	19	54.5	4.5	5.1	8.1	10.5	1.3	0.2	2.2	8.6	1.2	0.3	0.3	1.1	0.0	0.4	0.0	0.1	0.0	0.0	0.0	0.6	0.8	0.1	0.0	0.1	100.0
Palosco	2.1	3	142	4	34.2	0.9	4.6	8.0	40.1	0.3	1.9	0.3	4.9	0.0	0.2	0.2	1.6	0.1	1.0	0.0	0.0	0.0	0.0	0.0	0.6	0.9	0.1	0.0	0.1	100.0
Palosco	36.3	2	322	6	60.7	2.8	7.4	3.1	6.3	0.0	0.2	0.0	14.2	0.0	0.3	1.8	1.2	0.0	0.9	0.0	0.0	0.0	0.0	0.0	0.5	0.6	0.0	0.0	0.1	100.0
Palosco	41.2	0	124	1	28.7	0.4	1.4	14.8	22.9	0.0	0.9	1.3	29.2	0.0	0.0	0.0	0.5	0.0	0.0	0.0	0.0	0.0	0.0	0.0	0.0	0.0	0.0	0.0	0.0	100.0
Cremignane	35.2	2	164	5	23.0	0.1	4.4	8.5	45.3	2.5	4.7	1.0	7.4	0.0	0.2	0.8	0.6	0.0	0.9	0.1	0.0	0.0	0.0	0.0	0.2	0.3	0.0	0.0	0.0	100.0
Cremignane	54.5	0	137	17	18.7	0.6	3.2	7.0	56.6	0.0	4.3	2.2	6.5	0.0	0.2	0.2	0.4	0.0	0.1	0.0	0.0	0.0	0.0	0.0	0.1	0.1	0.0	0.0	0.0	100.0
Cremignane	74.5	0	76	17	26.3	0.3	3.4	4.9	30.5	26.8	1.7	0.0	4.7	0.0	0.9	0.0	0.3	0.0	0.1	0.0	0.0	0.0	0.0	0.0	0.0	0.0	0.0	0.0	0.0	100.0
P. Borromeo	9.8	2	355	22	52.2	9.0	19.0	0.3	2.2	1.2	0.6	1.6	9.6	0.3	0.8	0.2	0.9	0.1	0.8	0.0	0.2	0.0	0.0	0.0	0.4	0.6	0.1	0.0	0.0	100.0
P. Borromeo	51.8	1	357	2	50.7	4.3	16.4	1.2	0.0	0.0	0.0	0.0	20.4	0.3	2.8	2.8	0.3	0.0	0.3	0.0	0.1	0.0	0.0	0.0	0.2	0.2	0.0	0.0	0.0	100.0
P. Borromeo	102.8	3	333	7	53.0	6.5	14.2	0.6	0.0	0.0	0.9	0.3	13.6	2.5	1.2	3.1	1.2	0.1	1.2	0.0	0.1	0.1	0.0	0.0	0.5	0.7	0.1	0.0	0.0	100.0
Gaggiano	19.4	3	387	8	61.8	16.1	14.0	0.0	0.0	0.0	0.0	0.0	4.3	0.0	0.0	0.0	0.6	0.1	1.2	0.0	0.1	0.0	0.0	0.0	0.8	0.9	0.0	0.0	0.1	100.0
Gaggiano	44.5	5	338	17	51.7	13.4	17.1	2.2	0.0	0.0	0.0	0.6	7.5	0.0	0.5	0.5	1.7	0.1	1.8	0.0	0.1	0.0	0.0	0.0	0.8	1.7	0.1	0.0	0.2	100.0
Gaggiano	69.7	2	347	12	47.9	5.1	16.5	0.3	0.0	0.0	0.0	0.3	22.2	0.0	2.2	2.5	1.0	0.0	0.8	0.0	0.1	0.0	0.0	0.0	0.5	0.2	0.1	0.0	0.1	100.0
Gaggiano	101.3	1	410	16	41.8	10.8	13.6	0.3	0.0	0.0	0.0	0.6	7.7	0.3	7.7	16.1	0.2	0.0	0.2	0.0	0.0	0.0	0.0	0.0	0.2	0.3	0.0	0.0	0.0	100.0
Triulza	6.1	2	109	7	54.6	5.6	11.2	17.4	0.0	0.0	0.0	3.7	5.0	0.0	0.0	0.0	0.9	0.0	0.6	0.0	0.0	0.0	0.0	0.0	0.4	0.6	0.1	0.0	0.0	100.0
Triulza	20.5	2	350	13	60.6	3.4	18.3	1.6	0.0	0.0	0.0	2.8	8.4	0.3	0.6	0.9	1.0	0.0	1.0	0.0	0.1	0.0	0.0	0.0	0.7	0.1	0.1	0.1	0.0	100.0
Triulza	22.2	1	314	1	58.4	4.3	0.3	1.8	0.0	0.0	0.0	6.4	13.7	0.3	2.1	11.9	0.2	0.0	0.0	0.0	0.0	0.0	0.0	0.0	0.5	0.0	0.1	0.0	0.0	100.0
Triulza	38.5	3	358	20	53.4	3.1	18.4	1.2	0.0	0.0	0.3	0.3	17.7	0.3	0.5	0.8	1.6	0.1	0.7	0.0	0.0	0.0	0.0	0.0	0.9	0.4	0.3	0.0	0.1	100.0
Triulza	47.2	1	326	11	54.9	5.1	17.4	0.6	0.0	0.0	0.0	0.0	15.0	0.9	0.8	3.5	0.5	0.1	0.6	0.0	0.1	0.0	0.0	0.0	0.3	0.1	0.1	0.0	0.1	100.0
Triulza	57	4	380	8	48.3	6.4	14.6	0.0	0.0	0.0	0.0	0.0	15.8	0.9	2.6	5.6	1.7	0.0	0.9	0.0	0.0	0.1	0.0	0.0	0.5	1.6	0.9	0.0	0.1	100.0
Triulza	64.3	4	351	4	42.1	8.7	14.4	0.3	0.0	0.0	0.0	0.0	9.9	1.5	7.8	9.9	1.2	0.1	1.4	0.0	0.2	0.0	0.0	0.0	0.9	1.1	0.1	0.1	0.1	100.0
Triulza	69.5	3	337	12	48.5	9.7	11.5	1.5	0.0	0.3	0.0	1.2	14.6	1.8	2.3	3.2	2.2	0.1	1.1	0.0	0.3	0.0	0.0	0.0	1.1	0.2	0.3	0.0	0.1	100.0
Parco Nord	24.1	3	392	12	46.0	9.3	20.2	0.6	0.0	0.0	0.3	0.3	13.7	2.2	1.2	2.8	0.8	0.0	1.1	0.0	0.2	0.0	0.0	0.0	0.7	0.4	0.1	0.0	0.1	100.0
Parco Nord	43.4	2	383	2	51.1	7.2	17.1	0.0	0.0	0.0	0.0	0.3	13.7	1.2	1.9	4.1	1.0	0.1	0.9	0.0	0.2	0.0	0.0	0.0	0.7	0.2	0.2	0.0	0.1	100.0
Parco Nord	77.2	3	344	8	45.2	7.9	15.6	0.0	9.1	0.4	1.5	1.5	12.2	0.0	1.2	2.1	0.6	0.0	1.1	0.0	0.1	0.0	0.0	0.0	0.5	0.6	0.2	0.0	0.2	100.0

3.3 Principal components analysis

The principal component analysis (PCA) is a powerful tool for analysing data and it is a way of identifying patterns in data, and expressing the data in such a way as to highlight their similarities and differences (Frank and Todeschini, 1994). The PCA generates a new set of variables, called principal components. Each principal component is a linear combination of the original variables. All the principal components are orthogonal to each other, so there is no redundant information. The principal components as a whole form an orthogonal basis for the space of the data. Traditionally, principal components analysis is performed on the symmetric covariance matrix or on the symmetric correlation matrix. I consider the covariance matrix *S* where the variables of the original data matrix X have been autoscaled [Eq. (1)] to mean 0 and variance 1 (in this case, the covariance matrix of standardized matrix equals the correlation matrix of original data).

1) $x'' = \frac{x_{ij} - \bar{x}_j}{s_j}$

Let *Xc* be the autoscaled matrix (Table 2) where *n* row corresponds to different samples and *p* column corresponds to one of several different variables. To compute the principal components, the matrix of eigenvalues *Λ* (*p, p*; Table 3) and its corresponding eigenvector-loading matrix *L* (*p, M*; Table 4) are calculated diagonalizating the covariance matrix *S* of *Xc*,

2) $diag(S) = diag\left[\frac{Xc^T Xc}{n-1}\right]$

Each eigenvector defines a principal component. A component can be viewed as a weighted sum of the conditions, where the coefficients of the eigenvectors are the weights. Now is possible to represent the data matrix *X* in a new orthogonal space,

3) $T = XcL$

where *T* = scores matrix (*n, M*, Table 5)

K correlation index (Todeschini, 1997) has been used to evaluate the total quantity of correlation contained in the data set,

4) $$K = \frac{\sum_{q=1}^{p} \left| \frac{\lambda_q}{\sum_{q=1}^{p} \lambda_q} - \frac{1}{p} \right|}{\frac{2(p-1)}{p}}$$

The variance accounted for by each of the components is its associated eigenvalue. Consequently, the eigenvectors with large eigenvalues are the ones that contain most of the information; eigenvectors with small eigenvalues are uninformative.The sum of all eigenvalues represents the whole variance presents in the data. The variance explained by the first principal components is,

5) $EV_1\% = \frac{\lambda_1}{\sum_{q=1}^{p} \lambda_q} .100$

Therefore, let *q* be the number of significative components (eigenvectors with large eigenvalues), the variance accounted by the *q* components will be,

6) $C.E.V.\% = EV_1 + ...+ EV_q$

Usually the eigenvectors with small eigenvalues (noisy components) are eliminated. However eliminating low variance components, while reducing noise, also discards information. Based on the K index, I chose to use the *KL* and *KP criterion* (Todeschini, 1997) to decide how many principal components (upper and lower limit respectively) should be retained in order to account for most of the data variability. In particular, these two functions, seem to be useful to estimate those components which contain a quantity of information greater than the noise (Table 3).

7) $KL = 1 + \mathrm{int}\left[(p-1)(1-K)\right]$

8) $KP = \mathrm{int}(p^{(1-K)})$

Where *int* denotes the greater of the nearest integer.

Principal components analysis also provides insightful graphical summaries with ability to include additional information as well. The loading plot analyze the importance of each variable in the different components and their direct-inverse correlation. The score plot analyze the sample's behavior in the different components and their similarity.

Table 2. Autoscaled matrix of the original data.

core	depth	tHMC	MI	HCl	quartz	k-feldspar	plagioclase	volcanic lithic grains	limestone	dolostone	siltstone	chert	metamorphic lithic grains	serpentinite	muscovite	biotite	opaques	apatite	hornblende	glaucophane	tremolite	clinopyroxene	orthopyroxene	spinel	epidote	garnet	staurolite	andalusite	sillimanite
Ghedi	26.3	-0.9	-1.9	0.5	-2.2	-1.1	-1.1	0.8	0.8	3.1	1.8	1.8	-1.6	-0.3	-0.6	-0.7	1.0	-0.8	-0.7	-0.4	-0.8	-0.4	-0.4	-0.1	-1.0	-0.8	-0.7	-0.2	-0.7
Ghedi	35.9	0.8	-1.4	-0.4	-0.6	0.0	0.3	0.7	0.0	0.8	1.0	-0.1	-1.3	0.1	-0.4	-0.4	1.3	0.3	2.7	-0.4	-0.9	1.9	-0.4	-0.1	-0.3	-0.5	-0.5	-0.3	-0.8
Ghedi	47.9	-0.5	0.2	-0.4	1.5	-0.7	-0.9	-0.5	-0.3	-0.4	0.0	-0.4	0.8	-0.7	-0.5	-0.4	0.1	-0.4	-0.7	0.1	-0.5	-0.6	-0.4	-0.1	-0.7	-0.1	-0.3	0.1	-0.2
Ghedi	49.6	-0.3	-0.6	1.7	0.2	-0.8	-0.6	2.5	-0.5	0.1	-0.3	-0.4	0.2	-0.7	0.0	-0.6	1.0	3.4	-0.8	3.2	-0.8	-0.4	0.6	-0.1	-0.1	0.0	-0.7	-0.3	-0.1
Ghedi	59.6	-0.4	-0.2	-0.3	0.7	-0.9	-0.9	0.6	0.2	-0.2	0.0	-0.6	0.2	-0.7	-0.3	-0.6	1.3	-0.7	-0.4	0.3	-0.4	-0.3	-0.4	-0.1	-0.6	-0.1	-0.4	-0.1	-0.5
Ghedi	71.8	-1.1	-1.6	1.2	-2.7	-1.2	-1.4	-0.3	1.8	4.1	-0.3	0.1	-1.8	-0.7	-0.5	-0.8	-1.4	-0.7	-1.0	0.2	-0.9	-0.5	-0.4	-0.1	-1.2	-0.8	-0.7	-0.3	-0.8
Ghedi	90.5	-0.5	0.1	1.3	0.7	-0.5	-0.3	-0.6	-0.7	-0.3	-0.3	-0.6	0.1	0.5	4.3	0.9	-1.0	-0.2	-0.5	3.5	1.0	-0.1	0.8	-0.1	-0.4	-0.7	-0.7	-0.1	-0.1
Pianengo	11.5	1.3	0.2	1.7	1.1	0.2	0.1	-0.2	-0.6	-0.3	-0.3	-0.6	-0.2	1.6	-0.6	-0.5	1.8	0.4	1.0	-0.4	0.2	3.8	1.8	-0.1	0.7	1.0	0.7	-0.1	3.4
Pianengo	38.3	-0.7	-0.6	0.0	1.0	0.0	0.1	-0.1	-0.5	-0.4	1.3	-0.6	-0.1	-0.7	-0.1	-0.4	-0.9	-0.8	-0.4	-0.4	-0.8	-0.5	-0.4	-0.1	-0.8	-0.5	-0.7	-0.1	-0.5
Pianengo	39.9	1.1	-0.1	-0.1	-0.4	-0.5	0.2	0.2	0.5	0.0	-0.5	-0.6	-0.3	-0.3	-0.1	-0.1	0.5	-0.4	1.9	-0.4	-0.6	0.0	-0.4	-0.1	-0.1	0.1	-0.5	6.5	-0.2
Pianengo	44	0.0	-0.2	0.1	0.1	-0.5	-0.3	0.1	-0.4	0.4	0.5	-0.6	1.1	-0.7	-0.1	-0.3	-0.1	-0.6	0.1	-0.4	-0.6	0.5	0.8	-0.1	-0.3	-0.2	0.7	1.6	0.2
Pianengo	63	-0.9	-1.0	0.6	-2.0	-1.1	-1.4	0.2	1.6	3.0	0.5	-0.1	-1.5	-0.7	-0.7	-0.8	-1.1	-0.7	-1.0	-0.4	-0.9	-0.5	0.1	-0.1	-1.1	-0.4	-0.3	-0.3	-0.7
Pianengo	80.6	-0.7	-0.6	0.0	-0.3	-0.9	-0.9	0.6	0.2	0.6	0.5	0.3	0.9	0.2	-0.6	-0.8	0.2	-0.7	-0.7	0.1	-0.4	-0.4	-0.4	-0.1	-0.8	-0.5	-0.4	-0.2	-0.4
Cilavegna	19.9	2.8	0.5	0.7	-0.6	0.6	1.8	-0.8	-0.6	-0.3	-0.7	-0.6	-0.7	-0.2	2.7	1.8	0.6	1.2	2.4	-0.4	-0.4	2.7	-0.4	-0.1	2.6	2.7	0.1	0.3	2.6
Cilavegna	61.8	2.9	0.7	1.1	0.4	0.2	1.0	-0.8	-0.7	-0.4	-0.7	-0.6	-0.4	1.3	1.0	0.5	0.9	0.7	2.4	-0.4	2.7	2.6	3.8	-0.1	2.3	3.3	0.8	-0.3	3.0
Cilavegna	61.8	2.7	1.4	1.1	0.5	0.7	1.3	-0.8	-0.7	-0.4	-0.7	-0.6	-0.8	-0.4	0.2	0.7	0.7	0.6	2.2	-0.4	2.5	2.5	3.6	-0.1	2.2	3.1	0.7	-0.3	2.8
Agrate	10.8	-0.7	-0.4	2.7	-1.0	1.9	0.4	-0.4	0.2	0.3	-0.2	1.2	-0.4	0.2	0.3	0.3	-0.8	-0.6	-0.5	-0.4	-0.6	-0.2	0.5	-0.1	-0.9	-0.7	-0.5	0.0	-0.6
Agrate	29.2	0.4	1.0	-1.0	-0.1	2.1	0.8	-0.8	-0.6	-0.4	-0.4	-0.6	-0.1	2.3	0.0	2.0	-0.6	3.7	0.7	-0.4	0.1	-0.4	-0.4	-0.1	0.0	-0.1	0.3	-0.3	0.2
Agrate	36.7	-0.9	-0.6	0.0	0.0	-0.3	-1.0	0.5	0.5	-0.4	0.4	5.0	-0.9	-0.3	-0.5	-0.5	-1.3	-0.8	-1.0	-0.4	-0.8	-0.5	0.0	-0.1	-1.1	-0.7	0.5	-0.1	-0.5
Agrate	42.5	0.3	0.6	0.4	0.2	1.9	0.0	-0.6	-0.7	-0.4	-0.7	-0.6	0.7	3.3	0.9	0.4	-0.1	0.2	0.4	-0.4	0.5	0.5	1.0	-0.1	0.2	0.2	-0.2	-0.2	-0.1
Trezzo	14.7	-1.1	-1.4	2.2	-0.5	-0.8	-1.2	3.4	0.1	-0.4	0.3	-0.4	2.0	-0.7	-0.6	-0.7	-1.0	-0.8	-1.0	-0.4	-0.9	-0.6	-0.4	-0.1	-1.2	-0.8	-0.6	-0.3	-0.8
Trezzo	21.4	-1.1	-1.6	1.4	-1.8	-0.9	-1.5	-0.2	2.8	-0.4	4.7	0.5	-1.0	-0.7	-0.6	-0.8	-1.3	-0.8	-1.1	-0.3	-0.9	-0.6	-0.4	-0.1	-1.2	-0.8	-0.6	-0.3	-0.7
Trezzo	45.7	-1.1	-1.5	-1.1	-0.8	-1.2	-1.4	1.4	1.5	-0.3	2.1	-0.6	0.1	-0.7	-0.3	-0.7	-0.6	-0.7	-1.0	-0.3	-0.5	-0.6	-0.4	-0.1	-1.1	-0.8	-0.6	-0.3	-0.7
Trezzo	54.6	-0.1	-0.6	0.4	0.8	-0.2	-0.8	0.7	-0.1	-0.3	-0.6	0.5	-0.4	0.8	-0.6	-0.7	0.4	-0.6	-0.6	1.1	0.5	-0.4	-0.4	-0.1	0.3	0.4	0.3	-0.1	-0.3
Palosco	2.1	0.2	-1.0	-1.2	-0.6	-1.0	-0.9	0.7	1.8	-0.4	0.2	-0.4	-1.0	-0.7	-0.6	-0.7	1.4	0.7	0.2	-0.4	-0.7	0.0	-0.4	-0.1	0.4	0.5	-0.3	-0.2	-0.2
Palosco	36.3	0.0	0.6	-0.9	1.3	-0.6	-0.4	-0.2	-0.3	-0.4	-0.6	-0.6	0.6	-0.7	-0.6	-0.2	0.5	-0.6	0.0	-0.4	-0.4	-0.4	-0.4	-0.1	0.3	0.1	-0.7	-0.2	-0.1
Palosco	41.2	-1.1	-1.2	-1.5	-1.0	-1.1	-1.4	2.0	0.7	-0.4	-0.2	0.1	3.1	-0.7	-0.7	-0.8	-0.9	-0.7	-1.1	-0.4	-0.9	-0.5	-0.4	-0.1	-1.2	-0.8	-0.7	-0.3	-0.7
Cremignane	35.2	-0.3	-0.8	-1.0	-1.4	-1.2	-0.9	0.8	2.1	-0.2	1.5	-0.1	-0.6	-0.7	-0.6	-0.5	-0.6	-0.5	0.0	4.3	-0.9	-0.4	-0.4	-0.1	-0.7	-0.4	-0.4	0.1	-0.8
Cremignane	54.5	-1.0	-1.0	0.2	-1.7	-1.1	-1.1	0.5	2.8	-0.4	1.3	0.5	-0.7	-0.7	-0.6	-0.7	-1.1	-0.4	-0.9	-0.4	-0.8	-0.5	-0.4	-0.1	-1.0	-0.7	-0.7	-0.3	-0.6
Cremignane	74.5	-1.1	-1.6	0.1	-1.2	-1.2	-1.1	0.1	1.2	2.2	0.1	-0.6	-1.0	-0.7	-0.4	-0.8	-1.1	-0.5	-1.0	-0.2	-0.8	-0.5	-0.4	-0.1	-1.1	-0.8	-0.6	-0.3	-0.7
P. Borromeo	9.8	-0.1	0.9	0.7	0.7	0.9	1.4	-0.8	-0.6	-0.3	-0.4	0.2	-0.2	-0.3	-0.4	-0.7	-0.1	0.5	-0.1	-0.4	1.7	-0.6	2.8	-0.1	0.0	0.0	-0.2	-0.2	-0.8
P. Borromeo	51.8	-0.7	0.9	-1.3	0.5	-0.2	1.0	-0.6	-0.7	-0.4	-0.7	-0.6	1.6	-0.3	0.4	0.0	-1.1	-0.4	-0.7	-0.4	-0.2	-0.5	-0.4	-0.1	-0.7	-0.6	-0.6	-0.3	-0.8
P. Borromeo	102.8	0.3	0.7	-0.8	0.7	0.3	0.6	-0.7	-0.7	-0.4	-0.2	-0.4	0.5	2.3	-0.2	0.1	0.5	0.3	0.5	-0.4	0.8	0.7	-0.4	-0.1	0.1	0.3	0.1	-0.1	-0.3
Gaggiano	19.4	0.5	1.2	-0.8	1.3	2.6	0.6	-0.8	-0.7	-0.4	-0.7	-0.6	-1.1	-0.7	-0.7	-0.8	-0.6	0.3	0.4	-0.4	0.2	0.0	-0.4	-0.1	1.1	0.6	-0.4	-0.3	0.6
Gaggiano	44.5	1.3	0.8	0.2	0.6	2.0	1.1	-0.4	-0.7	-0.4	-0.7	-0.3	-0.6	-0.7	-0.5	-0.6	1.5	0.8	1.2	-0.4	0.7	-0.3	-0.4	-0.1	1.0	1.8	-0.1	-0.3	0.8
Gaggiano	69.7	-0.2	0.9	-0.4	0.4	0.0	1.0	-0.8	-0.7	-0.4	-0.7	-0.4	1.9	-0.7	0.1	0.0	0.2	-0.5	-0.1	-0.4	0.5	-0.6	-0.4	-0.1	0.2	-0.5	-0.1	-0.3	0.6
Gaggiano	101.3	-0.8	1.4	0.1	-0.1	1.3	0.5	-0.8	-0.7	-0.4	-0.7	-0.3	-0.5	-0.3	2.3	3.9	-1.3	-0.7	-0.8	-0.2	-0.3	-0.5	-0.4	-0.1	-0.8	-0.4	-0.7	-0.3	-0.6
Triulza	6.1	-0.2	-1.3	-0.9	0.8	0.1	0.2	2.5	-0.7	-0.4	-0.7	1.2	-1.0	-0.7	-0.7	-0.8	-0.1	-0.8	-0.4	-0.4	-0.4	-0.3	-0.4	-0.1	0.0	0.0	0.3	-0.2	-0.5
Triulza	20.5	-0.1	0.9	-0.3	1.2	-0.4	1.3	-0.5	-0.7	-0.4	-0.7	0.8	-0.4	-0.3	-0.5	-0.5	0.1	0.0	0.2	-0.4	0.4	-0.4	-0.4	-0.1	0.8	-0.7	-0.2	0.4	-0.4
Triulza	22.2	-0.8	0.6	-1.5	1.1	-0.2	-1.5	-0.5	-0.7	-0.4	-0.7	2.5	0.5	-0.4	0.1	2.7	-1.3	-0.5	-1.1	0.2	-0.5	-0.6	-0.4	-0.1	0.1	-0.8	-0.1	-0.3	-0.3
Triulza	38.5	0.2	1.0	0.5	0.7	-0.5	1.3	-0.6	-0.7	-0.4	-0.5	-0.4	1.2	-0.4	-0.5	-0.5	1.3	2.0	-0.2	0.2	-0.6	-0.6	-0.4	-0.1	1.3	-0.2	1.2	-0.3	-0.1
Triulza	47.2	-0.4	0.7	-0.4	0.8	0.0	1.1	-0.7	-0.7	-0.4	-0.7	-0.6	0.7	0.4	-0.4	0.2	-0.8	0.4	-0.4	0.0	-0.2	-0.4	-0.4	6.8	-0.3	-0.7	-0.1	-0.2	0.6
Triulza	57	1.0	1.2	-0.8	0.4	0.3	0.7	-0.8	-0.7	-0.4	-0.7	-0.6	0.8	0.4	0.3	0.9	1.5	-0.5	0.1	-0.4	-0.7	0.1	-0.4	-0.1	0.3	1.6	5.7	-0.3	0.2
Triulza	64.3	1.0	0.9	-1.2	-0.1	0.8	0.7	-0.8	-0.7	-0.4	-0.7	-0.6	-0.2	1.1	2.3	2.1	0.5	1.3	0.7	-0.4	1.7	-0.3	-0.4	-0.1	1.4	0.8	0.3	0.2	-0.1
Triulza	69.5	0.5	0.8	-0.3	0.4	1.1	0.2	-0.5	-0.7	-0.4	-0.7	0.0	0.6	1.5	0.2	0.2	2.5	0.4	0.3	-0.4	2.4	-0.6	-0.4	-0.1	2.0	-0.6	1.2	-0.1	0.2
Parco Nord	24.1	0.2	1.3	-0.3	0.2	1.0	1.6	-0.7	-0.7	-0.4	-0.5	-0.4	0.5	2.0	-0.2	0.1	-0.2	-0.3	0.3	-0.4	1.7	-0.1	-0.4	-0.1	0.7	-0.2	-0.2	-0.3	-0.2
Parco Nord	43.4	0.1	1.2	-1.3	0.6	0.5	1.1	-0.8	-0.7	-0.4	-0.7	-0.4	0.5	0.8	0.0	0.4	0.2	0.2	0.1	-0.4	1.5	-0.1	-0.4	-0.1	0.7	-0.5	0.8	-0.3	-0.1
Parco Nord	77.2	0.2	0.8	-0.8	0.2	0.7	0.9	-0.8	-0.1	-0.4	0.1	0.2	0.2	-0.7	-0.2	-0.1	-0.5	-0.8	0.3	-0.4	0.0	-0.6	-0.4	-0.1	0.1	0.1	0.6	-0.3	0.7

Table 3. Eigenvalues, Eigenvalues Variance, Cumulative Eigenvalues Variance, K correlation index, KL and KP criterion.

ID	*Eigenvalue*	*E.V. %*	*C.E.V. %*	*K%*	*KL*	*KP*
1	9.734	34.8%	34.8%	*49%*	*15*	6
2	3.254	11.6%	46.4%			
3	1.934	6.9%	53.3%			
4	1.577	5.6%	58.9%			
5	1.364	4.9%	63.8%			
6	**1.159**	**4.1%**	**67.9%**			
7	1.148	4.1%	72.0%			
8	0.993	3.5%	75.6%			
9	0.936	3.3%	78.9%			
10	0.888	3.2%	82.1%			
11	0.831	3.0%	85.1%			
12	0.754	2.7%	87.8%			
13	0.655	2.3%	90.1%			
14	0.516	1.8%	91.9%			
15	**0.432**	**1.5%**	**93.5%**			
16	0.394	1.4%	94.9%			
17	0.323	1.2%	96.0%			
18	0.302	1.1%	97.1%			
19	0.199	0.7%	97.8%			
20	0.154	0.5%	98.4%			
21	0.147	0.5%	98.9%			
22	0.114	0.4%	99.3%			
23	0.087	0.3%	99.6%			
24	0.053	0.2%	99.8%			
25	0.032	0.1%	99.9%			
26	0.022	0.1%	100.0%			
27	0.000	0.0%	100.0%			
28	0.000	0.0%	100.0%			
Tot	*28*	*100.0%*				

Table 4 . Loading matrix for Po Basin cores. The eigenvector-loading matrix gives the weight of each variable for each principal component.

ID	*Variables*	*PC1*	*PC2*	*PC3*	*PC4*	*PC5*	*PC6*	*PC7*	*PC8*	*PC9*	*PC10*	*PC11*	*PC12*	*PC13*	*PC14*	*PC15*
1	tHMC	-0.2830	0.2202	0.0784	0.0475	-0.1228	0.0165	0.0575	0.0414	-0.0569	0.0454	0.0237	0.0056	-0.0280	-0.0500	-0.0380
2	MI	-0.2610	-0.2551	-0.0496	0.0609	0.0179	-0.0406	0.0242	0.0167	-0.0311	0.0408	-0.1865	-0.0529	0.1510	-0.0990	0.1470
3	HCI	0.0049	0.2891	-0.2447	-0.2691	0.2727	-0.1780	-0.0032	-0.2160	0.0219	-0.2732	0.0362	0.1545	0.4860	0.1780	-0.2040
4	quartz	-0.1920	-0.2657	0.2220	-0.1566	0.1529	-0.0829	0.1592	-0.1120	-0.2010	0.0951	-0.0287	-0.0793	-0.0530	0.3240	0.2380
5	k-feldspar	-0.2149	-0.1375	-0.1850	0.1962	0.1203	0.0479	-0.1235	-0.2719	-0.0221	0.1319	0.1324	0.2311	0.2420	0.1290	0.0780
6	plagioclase	-0.2619	-0.1014	-0.0048	0.1185	-0.0372	-0.1549	-0.1389	-0.0992	-0.0920	0.0443	-0.1207	0.0745	0.2170	0.0570	-0.1790
7	volcanic lithic grains	0.1880	0.1071	0.2605	-0.3280	0.0155	0.1026	0.0704	-0.1554	-0.0683	-0.0709	0.2943	0.2533	-0.1780	-0.1120	-0.2500
8	limestone	0.2414	0.2403	-0.0418	0.1128	-0.0977	0.0435	-0.0529	0.1789	0.0972	0.2402	-0.0197	-0.1480	0.1000	-0.2330	-0.0230
9	dolostone	0.1503	0.2343	-0.1855	0.1959	-0.0283	0.0055	-0.2706	-0.0632	-0.0048	-0.5011	-0.3152	0.0304	-0.2460	0.0110	0.1130
10	siltstone	0.2017	0.1921	-0.0269	0.0619	0.0106	0.0346	-0.0080	0.1979	0.1955	0.4547	0.1688	-0.1257	0.3450	0.1650	-0.1090
11	chert	0.1141	-0.0277	-0.0812	0.2215	0.3611	0.2109	0.3039	-0.1278	-0.4590	-0.0828	0.3710	-0.2226	-0.0610	-0.1370	-0.1310
12	metamorphic lithic grains	-0.0300	-0.3207	0.2661	-0.3038	0.0273	-0.1325	0.1321	0.1063	0.4332	-0.1360	0.0654	0.1442	0.0270	-0.2340	-0.0750
13	serpentinite	-0.1691	-0.0681	-0.1465	0.0254	0.0718	0.1704	-0.2809	-0.1201	0.4372	-0.1339	0.4770	-0.3131	-0.1310	0.0970	0.1850
14	muscovite	-0.1330	-0.0604	-0.4701	-0.2263	-0.2425	0.0799	0.2250	0.1407	0.0730	-0.0861	-0.0150	0.0275	-0.0550	0.1880	-0.3510
15	biotite	-0.1485	-0.1868	-0.4112	0.0453	-0.2066	0.1193	0.1895	0.2307	-0.0386	-0.0724	0.2170	0.1671	-0.0970	-0.1570	-0.0310
16	opaques	-0.1719	0.1569	0.3802	-0.0348	-0.0773	0.2894	-0.1574	-0.0539	0.0232	-0.1724	0.0043	-0.1063	0.0210	0.2690	-0.2850
17	apatite	-0.1616	0.0261	-0.0216	-0.2353	-0.1485	0.2359	-0.4758	-0.1038	-0.2085	0.0796	0.1761	0.2000	0.1640	-0.4490	0.1430
18	hornblende	-0.2455	0.2316	0.0719	-0.5748	-0.2485	-0.0651	0.0067	-0.1070	-0.0061	0.1199	0.1276	-0.0115	-0.0800	0.0830	0.0010
19	glaucophane	0.0547	0.0159	-0.1341	0.1158	-0.1786	0.2127	-0.0537	0.0787	-0.2793	0.0396	-0.1295	-0.3990	0.0690	0.1660	0.2400
20	tremolite	-0.2354	-0.0236	-0.0913	-0.0342	0.2134	0.0502	-0.0578	-0.1730	0.2168	0.1505	-0.2154	-0.3825	-0.2030	-0.1700	-0.3680
21	clinopyroxene	-0.1979	0.3324	0.0013	-0.0356	0.0383	-0.1185	0.1088	0.1355	0.1002	-0.0143	0.2576	0.0985	-0.2070	0.2340	0.2820
22	orthopyroxene	-0.1547	0.2525	-0.1205	-0.2127	0.3714	-0.1741	0.1408	-0.0806	0.0969	0.0143	-0.1002	-0.1810	0.0100	-0.3750	0.1780
23	spinel	-0.0115	-0.1274	0.0131	-0.0287	0.0305	-0.5867	-0.4086	0.3592	-0.2820	-0.1033	0.2655	-0.2298	-0.0580	-0.0020	-0.2430
24	epidote	-0.2853	0.0734	0.0816	0.0285	-0.0324	0.1303	-0.0249	0.0001	-0.1248	0.0778	-0.0975	-0.0455	-0.1050	-0.0610	-0.2970
25	garnet	-0.2466	0.2487	0.0651	0.0057	0.0060	0.0433	0.1306	0.1857	-0.0888	0.0533	-0.1018	0.1267	-0.0150	-0.1260	-0.0010
26	staurolite	-0.1449	-0.0365	0.2040	0.1600	0.1084	0.3012	0.0885	0.4393	0.0353	-0.4226	0.0046	-0.1567	0.4240	-0.0680	0.0590
27	andalusite	-0.0127	0.0698	0.0988	0.0898	-0.5393	-0.2962	0.3022	-0.3795	0.0002	-0.2083	0.1374	-0.3251	0.2330	-0.1910	0.0540
28	sillimanite	-0.2453	0.2273	0.0301	-0.0578	0.1066	-0.1750	0.0842	0.2323	-0.0670	0.0078	0.0517	0.0877	-0.0740	-0.0250	0.1050

Table 5. Score matrix for Po Basin cores. The eigenvector-score matrix gives the weight of each sample for each principal component.

core	*depth*	*PC1*	*PC2*	*PC3*	*PC4*	*PC5*	*PC6*	*PC7*	*PC8*	*PC9*	*PC10*	*PC11*	*PC12*	*PC13*	*PC14*	*PC15*
Ghedi	26.3	4.5882	2.5760	-0.5398	1.5361	0.4631	0.9379	-0.8755	-0.3169	-0.3242	-1.3060	0.2369	-0.3967	-0.6266	0.4985	-0.8992
Ghedi	35.9	0.1550	2.5948	0.7802	1.0332	-1.2243	0.3837	-1.0234	-0.5426	-0.0387	0.4784	1.3390	0.6056	-0.8823	1.5944	0.1369
Ghedi	47.9	0.9975	-1.3316	1.1622	-0.5767	0.0396	-0.3752	0.6561	0.1789	0.0080	0.2344	-0.7150	-0.0248	-0.0132	0.5148	0.8005
Ghedi	49.6	1.0321	1.0283	0.4797	-4.8347	-0.4066	1.4055	-1.6354	-0.9686	-1.8911	-0.5856	0.2176	0.7282	0.7833	-0.7852	0.2231
Ghedi	59.6	1.3554	-0.0965	1.4983	-0.7535	-0.3314	0.2209	0.2543	0.0953	0.0582	-0.0120	-0.5930	-0.0873	-0.3961	0.8905	-0.0801
Ghedi	71.8	5.0153	2.4610	-2.2654	1.2969	-0.0737	-0.1885	-1.4090	-0.0530	-0.1181	-2.0214	-1.7554	0.1476	-0.7328	-0.3247	0.4525
Ghedi	90.5	-0.4718	-0.9818	-3.9233	-3.9402	-0.7610	0.2299	1.0728	0.2033	0.1157	-0.3160	-0.8011	-1.5355	-0.0772	1.3729	-0.2959
Pianengo	11.5	-4.2308	3.4871	1.1033	-0.8841	1.6457	-0.7905	0.1522	0.3679	0.7524	-0.7016	1.4521	0.1796	-0.1834	1.2227	1.5723
Pianengo	38.3	1.6241	-0.8708	0.0991	0.0446	0.0836	-0.8809	0.4947	-0.1768	0.1621	1.0119	-0.2742	0.6454	0.5125	1.2307	0.3012
Pianengo	39.9	-0.3331	1.4546	1.2689	1.1437	-4.7523	-2.2005	1.9180	-2.6284	-0.0007	-1.1187	0.7810	-1.5743	0.9622	-0.8549	0.1222
Pianengo	44	0.3208	0.4996	0.9261	-0.1742	-0.5491	-1.1586	1.2381	0.0957	0.8061	-0.8906	-0.1806	-0.0577	0.6173	-0.2533	0.5104
Pianengo	63	4.3169	2.1335	-1.2466	1.1908	0.2329	-0.1996	-0.8944	0.3016	0.2059	-1.1310	-1.3077	0.1956	-0.3877	-0.5562	0.4817
Pianengo	80.6	2.4241	-0.1288	0.7460	-0.3897	0.4193	0.1274	-0.0241	-0.0154	0.7527	-0.4666	0.1248	-0.2058	-0.4423	0.2421	-0.0193
Cilavegna	19.9	-5.8519	2.8669	-1.4258	0.2447	-2.2989	-0.0918	0.8588	1.3951	-1.0624	0.0452	0.6336	1.9705	-0.2992	0.5157	-0.9128
Cilavegna	61.8	-7.2993	4.0451	-0.5686	-0.7830	1.4483	-0.5419	0.8062	0.6097	0.6415	0.3279	-0.1572	-0.7220	-0.8776	-1.0613	-0.1898
Cilavegna	61.8	-6.9410	3.6918	-0.3366	-0.3443	1.4874	-0.8840	0.9813	0.4878	-0.3558	0.7228	-0.9934	-0.0928	-0.3021	-1.1648	-0.0548
Agrate	10.8	1.1287	0.2121	-2.4521	0.4890	1.4083	-0.6327	0.2032	-1.4722	-0.0200	-0.8692	0.7070	0.8339	1.7236	0.4615	-0.3158
Agrate	29.2	-2.8589	-1.7371	-1.5374	0.5908	-1.0655	1.4542	-2.4409	-0.4538	0.1376	0.6135	1.7583	1.0267	0.5322	-1.5195	1.4633
Agrate	36.7	3.2020	-0.4695	-0.4305	1.4557	2.5060	0.8724	2.0673	-0.3965	-2.2713	-0.2523	1.9801	-1.0628	0.1455	-0.6008	0.0703
Agrate	42.5	-2.5400	-0.6987	-1.4378	-0.2652	0.6525	0.1755	-0.6593	-1.0139	2.0967	-0.3111	1.4543	-0.2292	-0.1841	0.2622	0.7193
Trezzo	14.7	3.8354	-0.0987	1.0510	-2.4160	0.9783	-0.8826	0.7656	-0.7118	1.2076	-0.8094	0.9775	1.9976	0.4157	-0.2209	-1.0627
Trezzo	21.4	5.4026	2.1274	-1.1100	0.8437	0.5654	-0.1437	0.0790	1.1905	1.1106	2.5768	0.8059	-0.5471	2.2575	0.2776	-0.6307
Trezzo	45.7	4.2391	0.3452	0.7001	-0.2118	-0.3131	0.0831	0.1668	0.8570	1.1334	1.5049	0.2743	0.0890	-0.3557	-0.2229	-0.3676
Trezzo	54.6	0.4134	-0.0219	0.7637	-0.7962	0.7549	0.9194	0.0964	-0.5333	-0.4227	-0.3921	0.1574	-1.0912	-0.3842	0.6798	-0.0725
Palosco	2.1	1.2636	1.6682	1.7479	0.3894	-1.1036	1.0045	-0.6454	0.6440	-0.4716	1.0461	-0.0251	0.1879	-0.6877	-0.5017	-0.3662
Palosco	36.3	-0.0482	-1.1373	1.4880	0.0160	-0.2457	-0.3653	0.4955	0.0234	-0.1574	0.4951	-0.9526	0.3341	-0.8517	0.3983	0.3447
Palosco	41.2	3.8357	-1.4628	1.9184	-1.1663	-0.0070	-0.3449	0.8233	0.5063	1.5461	-0.0459	0.5433	1.0798	-1.2869	-1.5023	-0.1370
Cremignane	35.2	3.6257	1.1557	-0.0868	-1.8259	-1.7599	1.0864	-0.1109	1.2045	-0.8703	1.5919	-0.3746	-1.9840	0.2256	0.0652	0.9979
Cremignane	54.5	4.3133	1.1184	-0.3271	0.5992	0.0919	0.0036	-0.0047	0.6630	0.3019	1.3410	0.3280	-0.0359	0.5100	-0.8543	-0.2630
Cremignane	74.5	4.0423	1.0846	-0.8211	0.5624	-0.2462	-0.3216	-0.8439	0.1165	0.2241	-0.7518	-1.1907	0.3714	-0.7014	-0.0475	0.4614
P. Borromeo	9.8	-1.6443	-0.3163	-0.4614	-0.1800	2.1040	-0.6744	-0.2965	-1.7456	-0.0371	0.5792	-1.4234	-0.7403	0.9308	-1.0969	-0.0768
P. Borromeo	51.8	0.2578	-2.9209	0.0684	-0.0572	-0.2886	-0.8176	0.3881	0.0434	0.6974	0.3314	-0.9377	0.6426	-0.4246	-0.2046	0.4838
P. Borromeo	102.8	-2.0910	-1.0271	0.3764	0.5013	-0.0991	0.4837	-0.8098	-0.3852	1.3341	0.1525	0.8307	-0.6902	-0.5894	0.5261	0.6612
Gaggiano	19.4	-2.2459	-0.8046	0.2900	1.2817	0.3628	-0.3748	-0.5000	-0.9654	-1.3340	1.5198	-1.0669	0.8928	0.2099	0.6569	0.9915
Gaggiano	44.5	-3.2275	0.5902	1.1448	0.7386	0.0947	0.3336	-0.7198	-0.9012	-1.2389	0.7692	-0.8500	0.9417	0.5982	0.4428	-0.6101
Gaggiano	69.7	-0.9845	-1.8896	0.7097	-0.1451	0.1304	-0.6647	0.4221	0.1942	0.6331	-0.0597	-1.1721	0.4792	0.0221	-0.0612	-0.5489
Gaggiano	101.3	-0.5688	-2.8109	-3.9629	0.3983	-0.9087	-0.1120	1.2968	0.4570	-0.2406	-0.0557	-0.0498	1.4851	0.0891	0.3461	-0.1836
Triulza	6.1	1.3271	-0.2728	1.7180	0.2552	0.8201	0.6021	0.8693	-0.8238	-1.6709	-0.1857	0.6773	0.5946	-0.9727	0.4503	-0.5595
Triulza	20.5	-0.8199	-1.2740	0.7588	0.7319	0.1869	-0.2455	0.2352	-1.1587	-1.1227	0.1802	-0.6353	-0.6013	0.0377	0.3073	-0.2446
Triulza	22.2	0.9053	-3.0011	-1.1993	0.5149	0.5132	0.8829	2.1547	0.7042	-1.4848	-0.1905	0.9508	-0.2365	-1.4013	-0.7412	0.7602
Triulza	38.5	-1.6446	-1.0336	1.7442	-0.7912	-0.1780	0.7886	-1.1877	0.1026	-0.6091	-0.6621	-0.7144	0.4810	1.5658	-0.3595	-0.1189
Triulza	47.2	-0.7587	-2.8129	0.1716	-0.3072	0.2825	-4.6126	-3.1812	2.4192	-1.7910	-0.6221	1.4966	-1.1777	-0.2577	-0.0078	-0.7126
Triulza	57	-3.1409	-0.9952	1.9000	1.3612	-0.0781	2.0400	0.8620	3.3127	0.5095	-2.6507	-0.2927	-0.1841	2.1503	0.1995	0.3900
Triulza	64.3	-3.6317	-1.2097	-1.6590	0.3696	-1.6902	1.3748	-0.2742	0.1844	0.4116	0.2521	0.1348	-0.1533	-0.7362	-0.6640	-1.2703
Triulza	69.5	-3.1077	-1.1365	0.9494	0.4557	0.3936	1.8133	-1.0340	-0.6997	0.9686	-0.5604	0.0106	-1.3823	-0.1356	0.1999	-1.6992
Parco Nord	24.1	-2.2959	-1.6040	-0.3690	0.7665	0.4559	-0.0214	-0.8728	-0.9976	1.3127	0.4426	-0.0597	-0.6486	-0.2809	0.3100	-0.2520
Parco Nord	43.4	-2.1612	-2.0308	0.2843	0.7764	0.0039	0.6032	-0.5246	-0.0016	0.6721	0.1652	-0.5160	-0.6377	-0.3417	-0.1503	-0.1109
Parco Nord	77.2	-0.7188	-0.9707	0.3118	1.2546	0.2546	-0.3018	0.5967	0.6109	-0.2785	0.5811	-0.8292	0.1891	0.5231	0.0900	0.1106

3.4 Similarity and Canberra distance

Similarity (s) is a fundamental and widely used concept. Similarity analysis is used to compare the objects and decide which ones should be clustered together (similar objects) and which ones should not. When evaluating similarity the most natural way to access similarity is to evaluate the distance (d) between the two objects (v and t) being compared. Among different types of statistical distances we chose to use the Canberra distance (ranging from 0 to 1; Lance and Williams, 1966), because it is sensitive to small changes close to zero.

$$9)\ d_{vt} = \sum_{j=1}^{p} \frac{\left| x_{vj} - x_{tj} \right|}{(x_{vj} + x_{tj})}$$

Because each element of the sum is comprises between 0 and 1,

$$10)\ d_{vt}\max = p$$

Where p = number of variables. Dividing Canberra distance by p, similarity between v and t objects will be,

$$11)\ s_{vt} = 1 - d_{vt}$$

In paleodrainage analysis, similarity metrics can be used to identify the best modern analogue for any sample of ancient sediment or sedimentary rock, by comparing detrital modes of modern river sands (database by Garzanti et al, 2004 and 2006) and Pleistocene core sediments.

4 Results

KP function indicates that the six first principal components should be retained in order to account for most of the data variability (67.9% of the total variance). If we selecting the four principal components (58.9% of the total variance, Figures 2 and 3), and taking into account the eigenvectors value for all the parameters analyzed, the most important parameters on the PC1 (34.8% of total variability) are: sedimentary lithic grains (limestone and siltstone), feldspars (plagioclase and k-feldspar), amphiboles (hornblende and tremolite), garnet, sillimanite, epidote, tHMC and MI. The most important contributions to PC2 (11.6% of total variability) are: metamorphic lithic grains, dolostone, quartz, pyroxenes and HCI. The third and fourth components explaining 12.5% of total variability (Fig. 4), and are characterized by volcanic and metamorphic lithic grains, muscovite, biotite, opaques and hornblende.

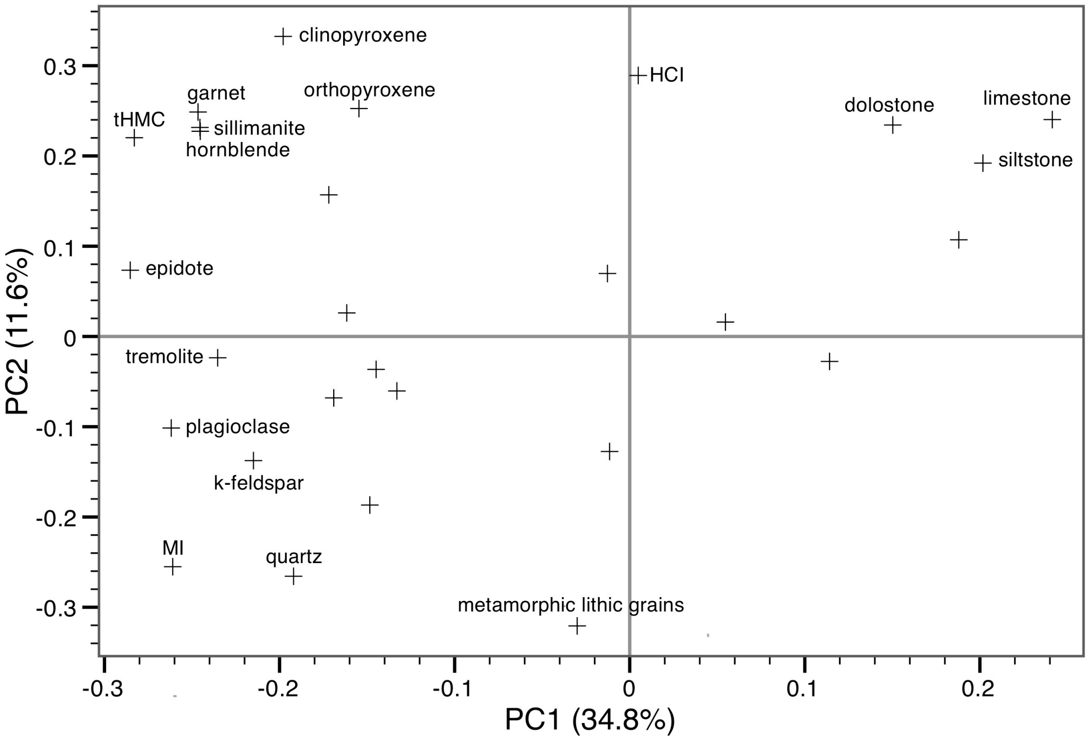

Figure 2: Principal components loading plot for the Po Basin cores. The first two principal components account for 46.4% of total variance, and are characterized by labelled grain-types.

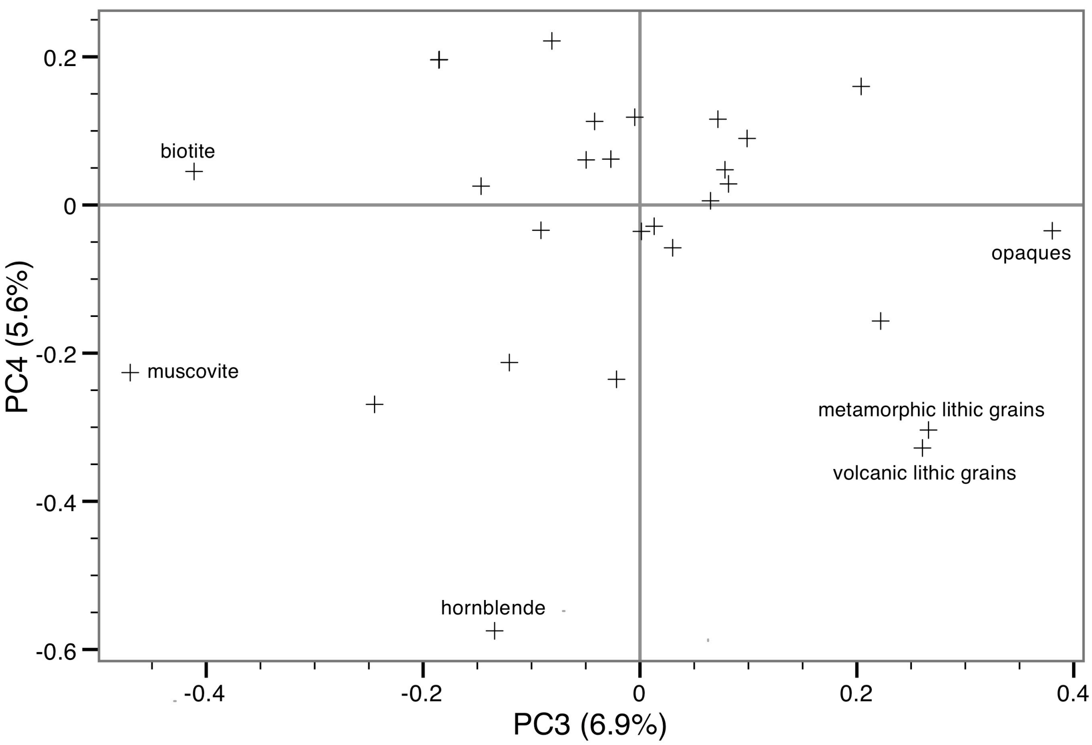

Figure 3: Principal components loading plot for the Po Basin cores. The third and fourth principal components account for 12.5% of total variance, and are characterized by labelled grain-types.

The results achieved by statistical analysis are shown in Figure 4, where PCA separates the samples studied into three different groups and a singleton:
1) *Group a*. These samples are characterized by sedimentary lithic grains and are located in the cores drilled in the eastern part of the Po Basin and near the Southalpine margin (cores RL1-Ghedi, RL5-Trezzo, RL6-Cremignane and RL7 Palosco) with the except for the core RL2-Pianengo (located more basinward). Similarity-metric analysis indicates that the petrographic composition of these samples, best compare with detritus of the modern Serio, Brembo and Oglio rivers. These rivers mainly run a course through the Mesozoic sedimentary successions of the Southalpine Domain. 2) *Group b*. Core samples are characterized by metamorphic lithic grains, quartz, feldspars and MI. These sediments belong to cores located around Milan (RL4 Agrate, RL8-Peschiera Borromeo, RL9-Gaggiano, RL10-Triulza and RL11 Parco Nord). Similarity analysis suggests that these sediments best compare with detritus of the modern Adda and Ticino rivers. Their catchments are located in the Central Alps and includes metamorphic rocks of the Austroalpine Domain and gneissic rocks of the Lepontine Dome. 3) *Group c*. Samples are characterized by hornblende, tremolite, garnet, sillimanite, epidote, pyroxenes tHMC and HCI and are located in the core RL3-Cilavegna (drilled in the western part of the Po Basin). Similarity-metric analysis indicates that these sediments best compare with detritus of the modern Sesia River, draining the mafic granulite rocks of the Ivrea-Verbano Zone (the deepest tectonic unit of the Southern Alps). 4) *Singleton*. The sample is characterized by hornblende, garnet, epidote, and HCI and is located in the core RL2-Pianengo. Similarity analysis indicates that the petrographic composition of this samples, best compare with detritus of the modern Oglio River,

which drains not only the Southalpine sedimentary successions, but also the tonalite-granodiorite rocks of the Oligocene Adamello Pluton.

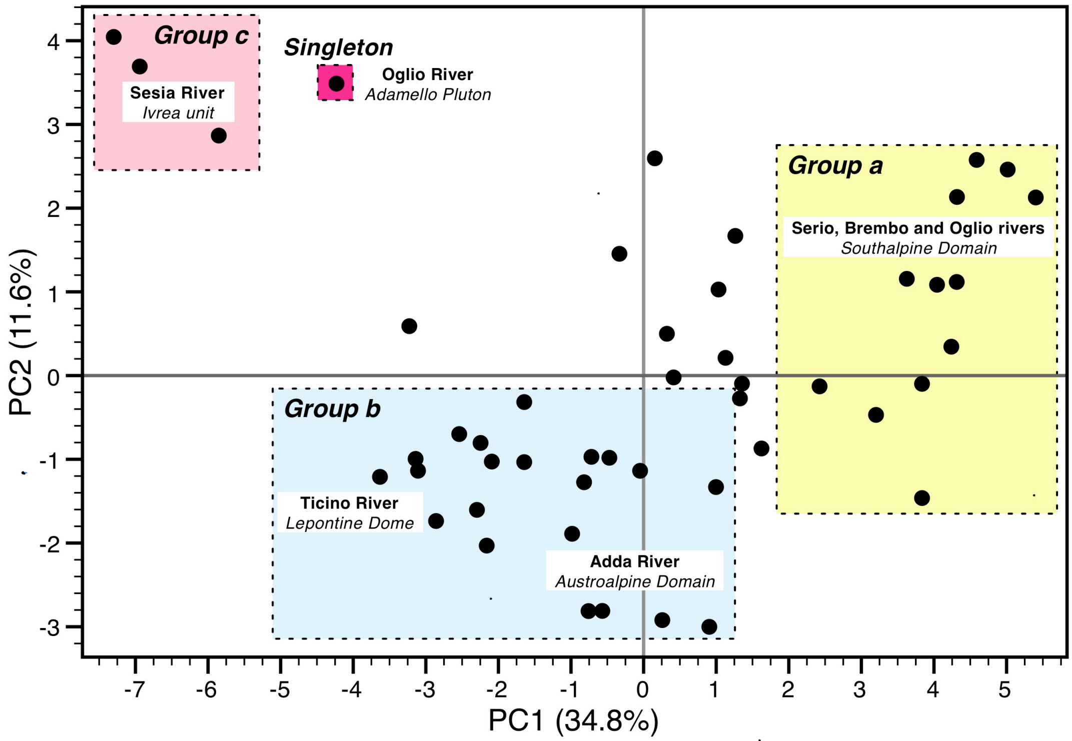

Figure 4: Principal components score plot and similarity analysis for the Po Basin cores.

5 Conclusion

In order to obtain a high-resolution Pleistocene stratigraphy, eleven continuously cored boreholes, 100 to 220m deep were drilled in the northern part of the Po Plain by Regione Lombardia in the last ten years. Quantitative provenance analysis (QPA, Weltje and von Eynatten, 2004) of Pleistocene sediments was carried out by using multivariate statistical analysis (principal components analysis and similarity analisys) on an integrated data set, including high-resolution bulk petrography and heavy-mineral analyses on Pleistocene sands and of 250 major and minor modern rivers draining the southern flank of the Alps (Garzanti et al, 2004; 2006).

QPA allowed us to tentatively reconstruct the major changes of patterns of paleodrainage and foreland-basin fills in the last 1 Ma. Prior to the onset of major Alpine glaciations, detritus from the Western and Central Alps was carried longitudinally parallel to the Southalpine belt by a trunk river (PaleoTicino River) and its tributaries (Vezzoli and Garzanti, 2008). This scenario rapidly changed during the marine isotope stage 22 (0.87 Ma), with the onset of the first major Pleistocene glaciation in the Alps (Muttoni et al, 2003). PCA and similarity analysis from core samples show that the longitudinal trunk river at this time was shifted southward by the rapid progradation of transverse alluvial river systems fed from the metamorphic and crystalline rocks of the Central Alps and from sedimentary rocks of the Southalpine Domain. East of Lake Maggiore, carbonate detritus increased as a result of enhanced erosion and transport along Southalpine valleys and of reduced chemical weathering under cold and dry climatic conditions.

Acknowledgements

The article benefited from careful revisions and constructive comments by E. Garzanti, D. Sciunnach, S. Andò, G. Muttoni, and G. Scardia. Study funded by Regione Lombardia.

References

Carcano, C. and Piccin, A. (2002). Geologia degli acquiferi padani della Regione Lombardia: *Firenze, SELCA (Società Elaborazioni Cartografiche s.r.l.)*, pp. 130.

Frank, I.E. and Todeschini, R. (1994). *The Data Analysis Handbook. Elsevier*. Holland.

Garzanti, E. and Vezzoli, G. (2003). A classification of metamorphic grains in sands based on their composition and grade. *Journal of Sedimentary Research 73*, 830-837.

Garzanti, E., Vezzoli, G., Lombardo, B., Andò, S., Mauri, E., Monguzzi, S. and Russo, M. (2004). Collision-Orogen Provenance (Western and Central Alps): Detrital Signatures and Unroofing Trends. *Journal of Geology 112,* 145-164.

Garzanti, E., Andò, S. and Vezzoli, G. (2006). The Continental Crust as a Source of Sand (Southern Alps cross-section, Northern Italy). *Journal of Geology 114,* 533-554.

Garzanti, E. and Andò, S. (2007). Heavy-mineral concentration in modern sands: implications for provenance interpretation. In: M. Mange & D. Wright (Eds.), *Heavy Minerals in Use*, Developments in Sedimentology Series, Vol. 58, pp. 517–545. Elsevier, Amsterdam.

Garzanti, E. and Malusà, M. (2008). The Oligocene Alps: Domal unroofing and drainage development during early orogenic growth. *Earth and Planetary Science Letters 268*, 487-500.

Ingersoll, R.V., Bullard, T.F., Ford, R.L., Grimm, J.P., Pickle, J.D. and Sares, S.W. (1984). The effect of grain size on detrital modes: a test of the Gazzi-Dickinson point-counting method. *Journal of Sedimentary Petrology 54*, 103-106.

Lance, G. N., and Williams, W. T., 1966, *Computer programs for classification, in Proceedings*, Australian National Committee on Computation and Automatic Control Conference, paper 12/3, pp. 304-306. Canberra.

Mange, A. and Maurer, H. F. W. (1992). *Heavy minerals in colour*. pp. 147. London, Chapman & Hall.

Muttoni, G., Carcano, C., Garzanti, E., Ghielmi, M., Piccin, A., Pini, R., Rogledi, S. and Sciunnach, D. (2003). Onset of major Pleistocene glaciations in the Alps. *Geology 31*, 989-992.

Suttner, L.J. and Basu, A. (1985). The effect of grainsize on detrital modes: a test of the Gazzi-Dickinson point-counting method-discussion. *Journal of Sedimentary Petrology 55*, 616–617.

Scardia, G., Muttoni, G., and Sciunnach, D. (2006). Subsurface magnetostratigraphy of Pleistocene sediments from the Po Plain (Italy): constraints on rates of sedimentation and rock uplift. *Geological Society of America Bulletin 118,* 1299–1312.

Todeschini, R. (1997). Data correlation, number of significant principal components and shape of molecules. The K correlation index. *Analytica Acta 348,* 419-430.

Vezzoli, G. and Garzanti, E. (2008). Tracking paleodrainage in foreland-basin sequences. *Geology,* submitted.

von Eynatten, H. (2004). Statistical modelling of compositional trends in sediments. *Sedimentary Geology 171,* 79-89.

Weltje, G.J. and von Eynatten, H. (2004). Quantitative provenance analysis of sediments: review and outlook. *Sedimentary Geology 171,* 1-11.

Weltje, G.J. (2004). A quantitative approach to capturing the compositional variability of modern sands. *Sedimentary Geology 171,* 59-77.

Zuffa, G.G. (1985). *Provenance of arenites*. Dordrecht, Reidel , NATO ASI Ser. C 148.